Daytime ionospheric TEC weather study over Latin America

E. Romero-Hernandez[1,2], C.M. Denardini[2], H. Takahashi[2], J.A. Gonzalez-Esparza[5], P.A.B. Nogueira[3], M.B. de Pádua[2], R.G. Lotte[2], P.M.S. Negreti[2], O.F. Jonah[7], L.C.A. Resende[2], M. Rodriguez-Martinez[6], M.A. Sergeeva[4,5], P.F. Barbosa Neto[2], V. de la Luz[4,5], J.F. Galera Monico[8], E. Aguilar-Rodriguez[5]

Esmeralda Romero-Hernandez, Clezio M. Denardini, esmeralda.romerohdz@uanl.edu.mx; clezio.denardin@inpe.br

[1]Universidad Autónoma de Nuevo León, Facultad de Ciencias Físico-Matemáticas, LANCE, Monterrey, Mexico

[2]Instituto Nacional de Pesquisas Espaciais, São José dos Campos, SP, Brazil

[3]Instituto Federal de Educação, Ciencia e Tecnologia de São Paulo, Jacarei, Brazil

[4]CONACyT, Instituto de Geofísica, Unidad Michoacan, Universidad Nacional

This article has been accepted for publication and undergone full peer review but has not been through the copyediting, typesetting, pagination and proofreading process, which may lead to differences between this version and the Version of Record. Please cite this article as doi: 10.1029/2018JA025943

Abstract.

The present work is the first of a two-part weather study of the ionospheric Total Electron Content (TEC), based on data collected by four ground-based Global Navigation Satellite System (GNSS) networks that cover the whole Latin America from the Patagonia to the north of Mexico. From the best of our knowledge, the maps presented here are the first TEC maps obtained using ground-based data that covers the entire Latin America region, which

Autónoma de México, Morelia, Michoacán,

Mexico

[5]LANCE, Instituto de Geofísica, Unidad

Michoacán, Universidad Nacional

Autónoma de México, Morelia, Michoacán,

Mexico

[6]Escuela Nacional de Estudios Superiores,

Unidad Morelia, Universidad Nacional

Autónoma de México, Mexico

[7]MIT Haystack Observatory,

Massachusetts Institute of Technology,

Westford, Massachusetts, USA

[8]Departamento de Cartografia,

Universidade Estadual Paulista, Presidente

Prudente, Brazil

represent an advance to the space weather monitoring and forecasting of the ionosphere. This work provides a qualitative and quantitative daytime analysis of the ionospheric TEC variation, which encompasses: (a) the response of TEC to the solar flux at midday; (b) the seasonal variation of TEC in different latitudinal ranges; and (c) the North-South asymmetry of TEC over Latin America. The response to the solar flux is based on day-to-day TEC variations during two periods of different solar activity conditions: 2011 (ascending phase) and 2014 (maximum). The approximations of meridional wind component derived from HWM-14 model and h_mF_2 obtained from International Reference Ionosphere (IRI) model were used. Equinoctial asymmetries with an opposite configuration in high and moderate solar activity were identified in the TEC variation. For 2011, it was related to the solar flux change. However in 2014, according to the h_mF_2 variation, the influence of neutral wind becomes dominant. Among the results, we highlight an absence of winter anomaly in the Norther hemisphere in 2014 and a stronger annual anomaly for latitudes under $-20°$.

Keypoints:

- Response of TEC to the solar flux over Latin America
- Seasonal variation of TEC over Latin America
- North-South asymmetries of TEC over Latin America during daytime

1. Introduction

The day-to-day variation of the ionosphere is influenced by different physical aspects related to the Sun (radiation flux and solar activity), space weather events (solar flares and coronal mass ejections), and thermospheric processes (neutral winds and wave-like disturbances). On a long-term scale, the ionosphere presents a seasonal variation that is mainly caused by changes in the atmospheric composition $[O]/[N_2]$ and photoionization rate controlled by the position of the subsolar point. As different authors have pointed out, however, this seasonal variation is complex and still not well understood. Based on the density peak of the F_2-layer (N_mF_2) and the ionospheric total electron content (TEC) measurements some anomalies have been reported [e.g., *Balan et al.*, 1997; *Tsugawa et al.*, 2007; *Zhao et al.*, 2007; *Liu et al.*, 2009; **?**, 2013].

Such anomalies correspond to winter anomaly (or seasonal anomaly), equinoctial anomaly (or semiannual anomaly), and annual anomaly (or December anomaly). The winter anomaly is associated with a higher electron density in winter than in summer. In the same way, the equinoctial anomaly corresponds to a higher electron density in equinoxes than in solstices. The annual anomaly is thought in terms of both hemispheres simultaneously, i.e., globally. In this case, it is identified using the N_mF_2 averaged for both hemispheres. Thus, the annual anomaly presents a higher electron density during December than in June. Additionally, a difference between the electron density during equinoxes (March and September) has been observed. This is referred to as equinoctial asymmetry and has been studied by different authors [*Balan et al.*, 1998; *Zou et al.*, 2000; *Ren et al.*, 2011; *Liu et al.*, 2010; *Chauhan and Singh*, 2010; *Chen et al.*, 2012; *Nogueira P.A.B.*, 2013; *Jonah*, 2013, @].

Different theories have been proposed in order to explain these anomalies. It is well known that electron density in the F_2-layer is determined by photoionization, chemical loss through chemical reactions (e.g. $O^+ + O_2$ and $O^+ + N_2$) and transport processes induced mainly by neutral winds. The later has been indicated as one of the mechanisms responsible for the formation of anomalies in the electron density. The neutral winds have influence on the height of the density peak of F_2-layer (h_mF_2). An equatorward wind will give rise to an upward plasma movement while a poleward wind will cause a downward movement of plasma along the magnetic field lines. Thus, any change in h_mF_2 will produce a change in N_mF_2, as the loss factor decreases with the increase height.

At equatorial latitudes, the eastward electric fields, produced at E-region by the dynamo effect, play a crucial role over the ionospheric electron density distribution. Here, the vertical drift ($\overrightarrow{E} \times \overrightarrow{B}$) drives the plasma to high altitudes, though eventually it is diffuse along the magnetic field lines to low latitudes by the action of gravity and pressure gradients. This phenomenon, called plasma fountain effect, results in two crests of electron density located around $\pm 15°$, feature known as the Equatorial Ionization Anomaly (EIA) [*Abdu*, 2005]. The EIA configuration, however, is not constant but it is influenced by the solar and thermospheric conditions. During solstices, the meridional neutral wind modulates the plasma fountain effect with a general interhemispheric flow from the summer to the winter hemisphere that affects the EIA morphology.

Indeed, the neutral winds were used to explain the semiannual anomaly. *Fuller-Rowell* [1998] proposed the effect of "thermospheric spoon", in which the interhemi-

spheric general circulation acts as a spoon in the summer hemisphere to better combine the thermospheric components, compared to equinoctial months. The consequence is a higher recombination rate (i.e., lower $[O]/[N_2]$) at solstice than at equinox. In the case of winter anomaly, it is reported to be more intense during high solar activity. *Burns et al.* [2014] explained that this pattern results from larger winter to summer changes in the thermospheric composition ratio in solar maximum than in solar minimum.

Complementary to the neutral wind theory, it has been found that the annual anomaly results from the differences between both hemispheres, north and south. For instance, *Gulyaeva et al.* [2014] studied the north and south hemispheric components of the annual global anomaly using TEC, N_mF_2 and h_mF_2 data collected from different satellites during 1969-1987. They analyzed the effects of land and sea and seismic activity to the north-south asymmetry. Their findings pointed out that the ionosphere over the sea is denser and presents a higher h_mF_2 than over the land.

The above-mentioned set of studies has been mostly based on radio-occultation, ionosonde data or model simulations. Hence, the aim of the present study is to analyze the day-to-day variation of the ionosphere in the northern and southern hemispheres over the Latin American sector. It is based on the daytime TEC variations measured on the ground during two years corresponding to two different phases of the solar cycle 24: 2011 (ascending phase) and 2014 (maximum). The analysis is focused on aspects such as the TEC dependence with the solar activity and with the seasons, as well as the latitudinal location of the receiver.

2. Observations and methods

GNSS data collected from a set of stations distribute over Latin America has been used. Stations over Mexico are part of GPS networks named National Seismological Service (SSN - Mexico), Trans-boundary, Land and Atmosphere Long-term Observational and Collaborative Network (TLALOCNet - Mexico). Data collected over Central America came from the Continuous Monitoring Network (COCONet - Central America). For the GNSS data over South America, we used the stations belonging to the Brazilian Network for Continuous Monitoring of the GNSS Systems (RBMC), the International GNSS Service (IGS - South America) and the Red Argentina de Monitoreo Satelital Continuo (RAMSAC). Detail on the location of the receivers and the extension of some of these networks can be found in *Denardini et al.* [2016]. Figure 1 shows the location of GNSS receivers employed in this analysis, where the blue-line is representing the magnetic equator in 2011.

2.1. TEC variation over selected stations

The estimate of TEC was made by using the methodology of the Space Weather Study and Monitoring Brazilian Program (*Estudo e Monitoramento Brasileiro de Clima Espacial* (Embrace)) at the *Instituto Nacional de Pesquisas Espaciais*, here referred to as TECMAP, whose estimate is based on the approximation of *Otsuka et al.* [2002]. The method uses both pseudoranges (P_1, P_2) and carrier phases (L_1, L_2) measurements to approximate the slant TEC. The VTEC is obtained by multiplying the slant TEC with the slant factor (that is, the ratio between the length of the ray path and the thickness of the ionosphere). Finally, each vTEC value is mapped over a shell placed at 300 km (intersection between the ray path of the satellite signal

and the shell). In order to reduce the leveling errors this method is only considering those satellites with an elevation angle above 30°. Details about this methodology can be found in *Takahashi et al.* [2016]. Recent methodologies related to the vTEC estimation can be reviwed in *Zhang et al.* [2018]; *Liu et al.* [2018].

TECMAP estimates vTEC with a time resolution of 10 min. Taking into account this resolution, an hourly average of vTEC was calculated at 12:00 LT for representing the noontime trend. To study the spatial and temporal variations of electron density, this hourly average TEC was estimated for the GNSS stations in Figure 1. Thus, an overview of TEC variation at noontime can be obtained along the periods of study. Afterwards, the monthly average TEC was calculated using magnetically quiet days only. The selection of the quiet days was based on the variation of the Dst, Kp and AE geomagnetic indices. Consequently, a day is considered magnetically quiet for the present study when the Dst $\leq$ -30 nT, ΣKp $\geq$ 24, and AE $>$ 500. In addition to these criteria, we also discard the GNSS data when the Dst index reached values higher or lower than two times its standard deviation with respect to its daily mean.

Figure 2 illustrates the resulting monthly average TEC maps during daytime, estimated using the GNSS stations of the networks mentioned above. From left to right, the panels correspond to March, June, September and December of 2011 (up) and 2014 (down), representing the TEC variation in equinoxes and solstices at 12:00 LT. These maps reveal solar activity, seasonal and hemispheric differences in TEC, which will be analyzed and discussed in the following sections. Thereafter, the climatology of TEC (referred to as the TEC trend) under quiet conditions is investigated. This was performed by analyzing the TEC variations at different GNSS stations during

the whole year of 2011 and 2014, but after removing the disturbed days. It is worth mentioning that in the final TEC variation curves those days removed were also interpolated in order to enhance the tendency. Moreover, a running average of 81-days was applied in order to eliminate the short-term variations that are not considered in this study. Figure 3 shows as example a set of annual TEC variation curves for 2011 and 2014. These correspond to two GNSS stations located in the northern hemisphere (MANA) and in the southern hemisphere (SMAR). The asterisks represent the average vTEC for each day at that specific time, and the solid-line is the average trend under quiet conditions, i.e., without magnetically disturbed days.

2.2. TEC variation with respect to the solar flux and seasonality

The dependence between the day-to-day TEC variations is analyzed in terms of the season and solar activity conditions. For this later, the solar radio flux at 10.7 cm (F10.7) has been used as a proxy of solar activity. The daily F10.7 data in solar flux units (sfu), where 1 sfu = $10^{-22} W m^{-2} H z^{-1}$, were obtained from NOAA. Based on the work of *Liu et al.* [2006], the P index $\rightarrow$ $P = \frac{(F10.7 + F10.7A)}{2}$ is employed as a solar proxy, since it can better represent the solar EUV variability. In this approximation, F10.7A is referred to as the 81-days running average of daily F10.7. The general properties of the two years based on solar radio flux variation are presented in Table 1. The columns correspond to year, phase of solar cycle, average F10.7, minimum of F10.7A, month of occurrence, maximum of F10.7A and month of occurrence. Additionally, the plots and linear correlations between both parameters, day-to-day TEC variation and P index, are shown in Figure 4.

3. Results and discussion

In the following sections, the results of the present work are shown and discussed in terms of the differences in the variation of the TEC observed in both hemispheres with respect to the solar activity. In addition, seasonal effects of the TEC variation over the Latin America are presented and discussed considering the hemispheric asymmetries. Henceforth, we refer to the northern and southern hemispheres as NH and SH, respectively.

3.1. TEC variation at two different phases of solar cycle

The variation of TEC along the two years in different phases of solar cycle 24, 2011 (ascending phase) and 2014 (maximum), was examined. From the TEC maps in Figure 2, some differences in the TEC level between both years can be distinguished, mainly in March, June and December. In both hemispheres, a higher TEC was registered in 2014 when compare to 2011. This is due to the normal background increment of the solar radiation flux during the maximum of the solar cycle (see Table 1 for detailed information on the averaged, minimum and maximum, F10.7A values observed during the pediod of the analysis). This was expected due to the electron density in the ionosphere is mainly linked to the photoionization process, that in turn is caused by the solar radiation flux (e.g. UV, EUV, Lymann-α and X-rays).

In addition to this result, it is possible to identify the presence of some NH-SH asymmetries in these maps, which suggests that the solar activity effect is different in the NH and SH. Observing the maps of Figure 2, one clearly sees a maximum in the TEC around the equator with decreasing values towards higher latitudes, but in and around the crest of the EIA. Since the SH in this map contributes with more land,

and therefore with more GNSS receivers to the map, it may induce the reader that the TEC is always higher in the SH than in the NH. For this reason, the discussion on the asymmetries in the TEC maps are performed by making use of the 81-days running average presented in the Figure 3 to have unbiased conclusions.

Analyzing the day-to-day TEC variation at noon in Figure 3, it is possible to identify that the TEC variation is characterized by two crests related to the maximum of ionization occurring during equinoxes. A minimum of TEC is observed in June-July months, which coincides with the minimum F10.7A for both phases of the solar cycle (see table 1). Comparing both years though, it can be noted that the TEC trend, especially at the crests, exhibits a different configuration and the electron density level changes in the two years, especially when looking from crest-to-crest. When taking just into account the TEC level around the season minimum (at June-July), it is notable that the TEC during 2014 is evidently higher than the TEC values obtained on 2011.

To evaluate the influence of solar radiation on the TEC variation, the relationship between the P index (described in the previous section) and the day-to-day TEC was analyzed. Then, an average-TEC variation was calculated for each year using a set of GNSS receivers at different latitude in a narrow longitudinal sector: UNPM (mlat=30.3°, mlon=-15.8°), MANA (mlat=21.7°, mlon=-14.8°), ACP1 (mlat=19.7°, mlon=-8.0°), RIOP (mlat=8.2°, mlon=-6.5°), AREQ (mlat=-6.4°, mlon=0.8°), IQQE (mlat=-11.1°, mlon=2.3°), SANT (mlat=-23.1°, mlon=1.5°) and ANTC (mlat=-27.2°, mlon=0.7°). Here, "mlat" and "mlon" are referred to as magnetic latitude and longitude, respectively. Three average-TEC curves were generated. The first

one corresponds to the average of all the data collected by GNSS receivers (called total average-TEC for simplification). The second one corresponds to northern TEC variation, which is calculated using the receivers in the north part (UNPM, MANA, ACP1, RIOP) only. Finally, the third one represents the southern TEC variation, that is calculated averaging the receivers set in the southern hemisphere (AREQ, IQQE, SANT, ANTC).

Figure 4 shows the correlation between P index and the three average-TEC curves for 2011 (left panels) and 2014 (right panels), indicating the correlation coefficient (R). The error bars correspond to the standard deviation of average TEC values. In the first case, i.e. considering to the total average-TEC versus P index (top panels), a higher correlation was found in 2011 (R=0.93) indicating that the TEC variation was mainly caused by effect of solar flux. The analysis for 2014, however, lead to a correlation under 0.5, revealing a poor correlation between the TEC and the solar flux. In other words, during high solar activity there may be another mechanism ruling the TEC over selected stations besides the solar flux. The middle and bottom panels in Figure 4 show the correlation analysis for the NH and SH separately. Here, we also observe higher correlations during 2011 when compared to those obtained for 2014, even in the NH the R-value was negative. This fact reinforces the conclusion that another mechanism may role the ionosphere dynamics during higher solar activity.

In addition to this conclusion, the correlation analysis for both solar activities revealed a strong hemispheric asymmetry, especially during the solar maximum. This implies that the thermospheric processes had a dominant role in the TEC variation during this year. It is important to highlight that the standard deviation (error

bars) was also greater during 2014, which indicates a stronger latitudinal variability of electron density in comparison to 2011 (e.g. see NH-SH panel in Figure 4). Such asymmetries will be discussed in more detail in the Section 3.3.

3.2. Over all Seasonal TEC variation at midday

The TEC maps on Figure 2 exhibit significant changes in the TEC level between equinox (March and September) and solstice (June and December) which reveals the seasonal behavior of TEC variation. This well-known seasonal effect is mainly due to the changes in the pattern of meridional wind circulation [*Arriagada et al.*, 1997; *Karpachev and Gasilow*, 2001; *Maruyama et al.*, 2008] which in turn is caused by the temperature gradient that makes the whole atmosphere to expand leading to the neutral wind generation. The relative movement of the Earth's axis with respect to the solar ecliptic leads to the displacement of the the subsolar point from the tropic of Cancer to the tropic of Capricorn and vice-versa. Therefore, it will lead to an unbalanced distribution of radiation that will produce a net meridional wind that will drag the ionosphere along with it. So, in addition to this ionization aspect, the interhemispheric circulation also changes with the different seasons. As a general result, the TEC is clearly less intense during the winter solstices, when the maps are dominated by the blue colors. In relation to the EIA, we can note that some plots on Figure 2 are not exhibiting this anomaly. For instance, the EIA is not perceptible in March-2011, June-2011, September-2011 and -2014, and December-2011 plots. This is an effect caused by the colar scale, since we used the same scale for all maps in order to compare them. During some months, especially for 2011, the TEC level was low making difficult the EIA identification. Also, it is important to mention that EIA

becomes stronger after noon (around 14:00 LT), then our maps cannot show the entire EIA configuration. Thus, considering separately these maps the EIA was observed in all months, with exception of June and September-2011 and 2014, where the single crest phenomenon was present [*Huang et al.* , 2014].

From the samples of TEC presented in the Figure 3, such seasonal behavior becomes more clear to identify. The TEC variation at noon during these two solar cycle phases (2011 and 2014) is characterized by two crests, one in March-April and another in October-November; and two minimums, one in June-July and another one in December. However, the pick values of the TEC level are different for March-April and October-November. This signature is referred to as the equinoctial TEC asymmetry, and it is the first time that it reported from GNSS ground based-networks stations in this sector. In the present example, such asymmetry appears with a different configuration. In 2011, the October-November TEC crest shows larger values of TEC than the March-April crest, while it happened to be the opposite case in 2014. Using the average-TEC variation estimated in Section 3.1, the difference between the two average crests in 2011 was 16.5 TECu which implies that during October-November the TEC level incremented 30.4% with respect to the average value in March-April. In 2014, this difference was 10.1 TECu which means that the TEC level was 18.7% higher during March-April crest than in October-November. From our analysis in reference to the correlation between P index and day-to-day TEC, it is possible to state that the annual TEC variations may be explained in function of solar flux changes in 2011. However, the negative correlation in the case of 2014 suggests that other processes must be involved in the development of this equinoctial asymmetry.

Different authors have studied the properties of this asymmetry and its relationship to the solar activity cycle. For instance, *Unnikrishnan et al.* [2002] analyzed the equinoctial anomaly on TEC at particular latitude (19° N) during high and low solar activity conditions. They found an opposite configuration of the equinoctial asymmetry and reported that October crest was higher for high solar activity and March crest for low solar activity. In a similar way, [*Kawamura et al.*, 2002] studied the yearly variation of mean daytime electron density in low solar activity period. Analyzing the electron density profile at different altitudes using the middle and upper (MU) radar observations, they found that March crest was predominant. Recently, *Chen et al.* [2012] and *Aggarwal et al.* [2014] investigated on these equinoctial asymmetries using N_mF_2 and TEC data during different solar activity conditions. In one hand, *Chen et al.* [2012] found that in TEC observations the March crest was dominating during low and high solar activity. On the other hand, *Aggarwal et al.* [2014] pointed out that N_mF_2 at noontime strongly depends on the solar activity, increasing with the solar activity. The discrepancies between these results reveal the complex behavior of the ionosphere electron density, which indicates a complex dependence on the solar activity.

3.3. Hemispheric dependence of Seasonal TEC variation at midday

According to the TEC maps on Figure 2, a strong difference between the TEC level in equinoxes and solstices was registered in the NH and SH in the two years. For June solstice of 2011, the TEC was low in most part of the Latin American sector, even in the NH where the subsolar point was located. Nonetheless, a big NH-SH TEC difference was found in December solstice, having that the SH presented the

highest TEC values and the change in the TEC level was faster from the SH to the NH (large NH-SH TEC difference). Such effect was reflected as a strong annual anomaly in the SH, which can be better visualized in the plots of Figures 3 and 5. Figure 5 shows the comparison of TEC variations for 2011 and 2014, estimated during magnetically quiet days at 12:00 LT for a set of GNSS receivers places in the right-side map. The R-values correspond to the linear correlation coefficients between the GNSS receivers enumerated in the same order as appear in the top left corner labels on the graphs. The GNSS receivers chosen for the present analysis were distributed in two longitudinal sectors covering different latitudes in the NH and SH. It was made in order to analyze both latitudinal and longitudinal variations. Indeed, we can also infer these hemispheric asymmetries from the correlation between P index and the three average-TEC (Figure 4). The correlations for 2014 show greatest values of standard deviation (error bars) of the NH-SH average-TEC variation. In the same way, the TEC anomalies present considerable differences in each hemisphere.

As it was expected, analyzing the average TEC variation for each hemisphere separately it was found that this seasonal variation of the TEC depends on latitude. As per the results on the graphs of Figure 5, the TEC level decreased as the latitude of GNSS stations increases. This well-known effect is also related to the position of subsolar point that remains at low latitudes causing that solar radiation flux to be reduced poleward. Despite the differences in amplitude, the linear correlations between these stations were high in both hemispheres, indicating that the seasonal pattern of the TEC variation remains. The only exception was on RIOP in 2014, most probably influenced by the data gap at the end of the year. This result is consistent with the

fact that these GNSS stations were confined in a narrow longitudinal band and strong variations related to magnetic storms were not considered. Significant longitudinal variations were not appreciated during these periods.

Another interesting aspect deal with the TEC estimated from the GNSS stations located southern than -25°. They presented a deeper minimum of TEC in June-July that, in turn, intensifies the annual and semiannual anomalies in this hemisphere. This effect is related to the position of subsolar point in the NH and the thermospheric circulation. It is well established that during the solstices the temperature gradient between both NH and SH produces an interhemispheric wind circulation. In this scenario, the plasma moves from summer hemisphere to winter hemisphere causing a decrement of F-peak height that, in turn, provokes a decrement of O/N_2 ratio.

From the comparison in Figure 5, it is also possible to identify the hemispheric assymetry. This is especially clear during 2014, when the equinoctial asymmetry was not so evident in the SH as in the NH. In the same way, the presence of winter anomaly was identified in the NH. It is interesting to note that this anomaly was only visible in 2011. Using the TEC differences estimated from the values reported in Table 2 we derive that for 2011 this anomaly was very weak ($\Delta TEC_{NH} = 5TECu$) while for 2014 it was absent ($\Delta TEC_{NH} = -1.1TECu$). Furthermore, the annual anomaly was identified in 2011 and 2014. However, in 2014 it was only present in the SH, being stronger at magnetic latitudes under $-20°$ (see Figure 5). Such fact highlights the hemispheric asymmetry once more. For 2011, these findings are in agreement with the results reported by *Sai Gowtam and Tulasi Ram* [2017]. They analyzed the occurence of winter and annual anomalies during the ascending phase of solar cycle

24 using data of the FORMOSAT-3/COSMIC. In the case of winter anomaly, their results point out that at low latitudes it just appears to the early morning to afternoon hours, while for mid latitudes it is almost absent. In other hand, the annual anomaly exhibits strong enhancements over the crest of SH EIA, which correspond to magnetic latitudes around $-20°$.

In addition to the above metioned, a time lag between NH and SH equinoctial crests was found. According to the results presented in the Figure 5, it can be noted that in the SH the crests are located near by the center of the March equinox (as it can be observed from the vertical dotted-line). This effect became more evident in those stations farther from the magnetic equator, as for example SANT and ANTC. The average time lag between the two hemispheres (i.e. the difference in days when both crests reach the maximum) was $\sim$ 40 days. This suggests that the crests in the SH are farther each other (i.e. larger temporal difference between crests), then the NH crest are closer each other (i.e. smaller temporal difference between crests). In this case, the average time lag between the two hemispheres was $\sim$ 12 days. The time lag may be also observed at October-November equinox. However, in that case it occurs nearer to the center of the September equinox (black dotted-line) in the NH than in the SH.

With respect to the dependence with the solar activity, the equinoctial asymmetries identified in the two years showed an opposite configuration in high and moderate solar activity; see Figures 3 and 4. Based on the results of Section 3.1, we assume that these anomalies can be explained in terms of solar flux variation (higher correlation between TEC and P index) for 2011. However, for 2014, the termospheric processes

had a major influence in the development of this TEC asymmetry. Additionally, the ionosphere can be influenced by dynamic forces such as the neutral winds. Moreover, its plasma distribution around the magnetic equator depends on the magnetic field configuration. In this sense, the neutral winds, that transport the ionosphere plasma along the magnetic field lines, may change the h_mF_2 which, in turn, affects the recombination processes and electron density, as proposed in previous studies on the equinoctial asymmetry that support the influence of the thermosphere processes [e.g., *Balan et al.*, 1997, 1998; *Fuller-Rowell*, 1998; *Unnikrishnan et al.*, 2002; *Chen et al.*, 2012].

Unnikrishnan et al. [2002] pointed out that the equinoctial asymmetries in the ionospheric electron density arise mainly from the corresponding asymmetries in the thermosphere that, consequently, may generate differences in the neutral winds and the equatorial vertical drift. So, we present Figure 6 that explores the influence of neutral winds on the TEC variation in each hemisphere. This figure summarizes the effects of solar radio flux and meridional wind component on the TEC variation. The different panels correspond to the TEC variation in the NH and SH, daily F10.7 and its 27-day running average (red-line) in 2011 and 2014, and the meridional component of neutral wind in the two hemispheres. Here six GPS stations at magnetic conjugate points, simulating the TEC variations in the NH and SH, were used (see the map on the right side). The meridional neutral wind component was approximated using the newest version of the Horizontal Wind Model (HWM-14) [*Drob et al.*, 2015]. It has some limitations as no solar activity dependence, which means that no differences between the wind trend in different years can be identified; nonetheless, HWM-14 is able

to represent the wind variations of middle and upper atmosphere in a good manner. For that reason, we are including just one variation plot of meridional wind (labeled as "merdl") component for the two years; see panel 5 in Figure 6. Theoretically, magnetic conjugate points are defined as two points on Earth's surface, connected by a magnetic field line. In this scenario, the effects on the plasma at these points, caused in this case by the neutral wind drag, would be linked, i.e., the plasma, following the magnetic field lines, will be moved upward or downward depending on the wind direction and hemisphere. Consequently, this effect could be interpreted as a change in the electron density.

Observing the panel 5 in Figure 6, we see that the meridional wind component at the two conjugate points was negative most of the year (black- and green line), which means that the neutral wind was blowing to the south direction. Note that during May-June its magnitude was larger than in the other months, especially at the southern conjugate point. According to this thermospheric drag or circulation, the lowest electron density should be present in the southern conjugate point during these months (decrement of h_mF_2). Following the same idea, we can explain the lower TEC values during January-February and November-December in the NH. In these months, meridional wind was blowing to the NH. It means that the altitude of F2-peak decreased (decrement of h_mF_2) and therefore, the electron density also decreased in the NH (see Figure 6). For the SH, the meridional component was zero during these months, which resulted in a slow TEC difference with respect to the equinox or maximum TEC (low rate of TEC change) as compared to the NH. On the other hand, Figure 7 illustrates the daily variation of the F_2-layer peak height (h_mF_2) at 12:00 LT

during 2011 and 2014, using data from the International Reference Ionosphere model of 2012 (IRI-2012) [*Bilitza et al.*, 2014]. This approximation was made for an altitud of 350 km, based on a Chapman model. Each segmented-line represents the h_mF_2 variation at one particular geographic latitude (±38°, ±30°, ±25°, ±20°, ±15°, ±10°, ±5°, 0°) in a similar longitudinal sector to that one of the GNSS stations considered in Figure 6. The colors represent the NH (green), SH (blue), and the geographic equator (black). A latitudinal effect can be distinguished from these plots, i.e., h_mF_2 decreases with the increment of latitude. Such h_mF_2 variability corroborates with the argumentation based on the vertical plasma displacements for each year. During May-September we note an inverse configuration between both NH and SH altitude of F2-peak, finding that in these months the SH presented the minimum altitudes, which suggests a higher recombination rate in comparison to the NH. This fact is in agreement with the low TEC registered in the SH during this period (see Figure 5).

In order to better appreciate such discussion on these figures we present the average values of h_mF_2 at the conjugate points during equinoctial and solstitial months in the Table 2, where it is showed a comparison of both TEC- and h_mF_2-average during the months associated with the maximums and minimums of TEC (March-April, June-July, October-November and December) in 2011 and 2014, obtained at the conjugate points. Here, the TEC variation can be examined in terms of h_mF_2 change. Thus, we found a correlation between TEC and h_mF_2, having that low values of h_mF_2 are associated with low values of TEC. The TEC differences between the two hemispheres are very small during equinoxes (March-April and October-November). However, during solstices (June-July and December), we perceive an inverse change in the two hemi-

spheres as was expected, finding that the TEC was higher (larger h_mF_2) in summer hemisphere while it was lower in the other one.

In the same way, analyzing the TEC differences (ΔTEC) between March-April and October-November equinoxes we can distinguish the equinoctial asymmetries. TEC value in 2011 was higher for October-November equinox than March-April equinox, while for 2014, March-April equinox presented a higher TEC value. Also, hemispheric asymmetries can be perceived at these conjugate points. For 2011, equinoctial asymmetry was more noticeable in the southern point, and for 2014, it was visible at the northern point. Based on these approximations, we found that a decrease of F_2-peak height (h_mF_2 under 300 km) can produces a considerable decrease of TEC.

Finally, the influence of meridional wind over TEC variation may be verified comparing both h_mF_2 and the meridional wind component (see Figures 6 and 7). For instance, we observe that a meridional wind blowing towards the SH, i.e. during June-July, produces a rise of F_2-peak height in the NH and a fall in the SH, which is related to a TEC decrement in the SH. During December, when the meridional wind was blowing northward, lower values of h_mF_2 were registered in the NH while the SH presented larger values of h_mF_2. It was attributed to the meridional wind component blowing to the north.

4. Conclusions

We presented a climatological analysis of TEC over the Latin America region. Two years in the solar cycle 24, 2011 and 2014, were examined in order to analyze the solar activity influences, seasonal variations and hemispheric asymmetries of TEC. The main results are listed as follow:

• Higher correlations between TEC and P index were found during 2011. Nevertheless, no correlation was observed in NH during 2014, implying an hemispheric asymmetry.

• Equinoctial asymmetries with an opposite configuration in high and moderate solar activity were found. It can be explained in terms of solar flux variation for the observations made in 2011. Moreover, the analysis revealed significant differences between NH and SH equinoctial asymmetries, making evident the hemispheric asymmetries.

• Based on meridional wind approximations some seasonal features of the TEC variation may be explained; however, HWM-14 model cannot be used to interpret the TEC variation in 2014 due to its no solar activity dependence.

• A relationship between both TEC and h_mF_2 was observed in the two years. Any drop of h_mF_2 was manifested as a diminution of TEC (higher recombination rate).

• The TEC maps of the present work could cover the whole Latin America, from Mexico to Argentina, which will be employed as a monitoring tool for developing space weather studies.

Acknowledgments.

E. Romero-Hernandez thanks the postdoctoral fellowship by CONACyT and the *Posgrado en Ciencias de la Tierra*, UNAM. C. M. Denardini thanks CNPq/ MCTIC (grant 303643/2017-0). J.A. González-Esparza acknowledges support from CONACYT LN 293598, CONACYT PN 2015-173, CONACYT-AEM 2017-01-292684 and DGAPA-PAPIIT IN106916. Laysa C. A. Resende thanks to FAPESP (grant 2014/11198-9). P. F. Barbosa Neto thanks to

CAPES/MCTIC (grant 1622967). E. Aguilar-Rodriguez thanks DGAPA-PAPIIT project (grant IN101718), and CONACYT project (grant 220981). The authors thank Embrace/INPE for distributing the GNSS data, World Data Center for Geomagnetism, Kyoto, for the AE and Dst indices data, and NOAA for the Kp index and solar radio flux data [//ftp.swpc.noaa.gov/ pub/indices/]. The GNSS ground-based receiver data were collected from different GNSS networks in South America: RBMC from IBGE [ftp://geoftp.ibge.gov.br/informacoes _ sobre _ posicionamento _ geodesico/rbmc/dados/], RAMSAC of Argentina [http://www.ign.gob.ar/NuestrasActividades/Geodesia/Ramsac/DescargaRinex], IGS [ftp://garner.ucsd.ed and Central America: COCONET [http://coconet.cimh.edu.bb/ coconetgsac/gsacapi/file/form]. We thank these network sites for providing the data continuously.

GPS Rinex data for the Mexican region were obtained from the following GPS permanent networks: the Mexican Servicio Sismológico Nacional (SSN), IGEF-UNAM, SSN-TLALOCNet and TLALOCNet [http://tlalocnet.udg.mx/tlalocnetgsac/gsacapi/file/form]. The calculations of the local TEC values are partly based on GPS data provided by the Servicio Sismológico Nacional (SSN, 2018; Pérez-Campos et al., 2018) and the Transboundary, Land and Atmosphere Long-term Observational and Collaborative Network (TLALOCNet; Cabral-Cano et al., 2018) and SSN-TLALOCNet operated by the Servicio de Geodesia Satelital (SGS) and SSN at the Instituto de Geofisica-Universidad Nacional Autonoma de Mexico (UNAM) and UNAVCO Inc. We gratefully acknowledge all the personnel from SSN, SGS and UNAVCO Inc. for station maintenance, data acquisition, IT support and data distribution for these networks. TLALOCNet, SSN-TLALOCNet and related SGS operations are supported by the National

Science Foundation Number EAR-1338091, NASA-ROSES NNX12AQ08G, CONACyT projects 253760, 256012 and 2017-01-5955, DGAPA-PAPIIT projects IN104213, IN111509, IN109315-3, IN104818-3, and supplemental support from UNAM-Instituto de Geof sica and Centro de Ciencias de la Atmosfera. We thank the LACIGE-UNAM at ENES unidad Morelia for the data provided by GPS receiver, acquired through infrastructure CONACyT grant: 253691, and and also the UNAM-PAPIIT project IA 107116.

References

Abdu M.A.: "Equatorial ionosphere-thermosphere system: electrodynamics and irregularities", *Adv. Space Res.*, 2005, **35**: 771-787.

Arriagada M.A.,Foppiano A.J. and Buonsanto M.J.: "Solar activity variations of meridional winds over King George Island, Antarctica", *Journal of Atmospheric and Solar-Terrestrial Physics*, 1997, **59**(12): 1405-1410, https://doi.org/10.1016/S1364-6826(96)00178-2.

Aggarwal M., Bardhanb A., Sharma D.K.:"Equinoctial asymmetry in ionosphere over Indian region during 2006-2013 using COSMIC measurements", *Adv. Space Res.*, 2014, **60**: 999-1014.

Balan N., Y. Otsuka and S. Fukao: "New aspects in the annual variation of the ionosphere observed by the MU radar", *J. Geophys. Res.*, 1997, **24**(18): 2287-2290.

Balan N., Y. Otsuka, G.J. Bailey and S. Fukao: "Equinoctial asymmetries in the ionosphere and thermosphere observed by the MU radar", *J. Geophys. Res.*, 1998, **103**(A5): 9481-9495.

Balan N., Otsuka Y., Fukao S., Abdu M. A., Bailey, G. J.: "Annual Variations of the Ionosphere: A Review Based on MU Radar Observations", *Adv. Space Res.*, 2000, **25**(1): 153-162, doi: 10.1016/S0273-1177(99)00913-8.

Bilitza D., Altadill D., Zhang Y., Mertens C., Truhlik V., Richards P., McKinnell L.A., and Reinisch B.: "The International Reference Ionosphere 2012 - a model of international collaboration", *J. Space Weather Space Clim.*, 2014, **4**(A07): 1-12, doi:10.1051/swsc/2014004.

Burns A.G., Wang W., Qian L., Solomon S.C., Zhang Y., Paxton L.J., Yue X.: "On the solar cycle variation of the winter anomaly", *J. Geophys. Res. Space Phys.*, 2014, **119**: 4938-4949. http://dx.doi.org/10.1002/2013JA019552.

Cabral-Cano E., X. Prez-Campos, B. Mrquez-Aza, M. A. Sergeeva, L. Salazar-Tlaczani, C. DeMets, D. Adams, J. Galetzka, K. Feaux, Y. L. Serra, G. S. Mattioli, and M. Miller: "TLALOCNet: A Continuous GPS-Met Backbone in Mexico for Seismo-tectonic, and Atmospheric Research", *Seismological Research Letters*,2018, **89**(2): 373-381,doi: 10.1785/0220170190.

Chauhan V. and Singh O.P.: "A morphological study of GPS-TEC data at Agra and their comparison with the IRI model", *Adv. Space Res.*, 2010, **46**: 280-290.

Chen C.H., J.Y. Liu, K. Yumoto, C.H. Lin and T.W. Fang: "Equatorial ionization anomaly of the total electron content and equatorial electrojet of ground-based geomagnetic field strength", *Journal of Atmospheric and Solar-Terrestrial Physics*, 2008, **70**: 2172-2183.

Chen Y., Liu L., Wan W. and Ren Z.: " Equinoctial asymmetry in solar activity variations of NmF2 and TEC", *Ann. Geophys.*, 2012, **30**: 613-622, doi:10.5194/angeo-

30-613-2012.

Denardini C.M., Dasso S., Gonzalez-Esparza J.A.: "Review on Space Weather in Latin America. 2. The Research Networks Ready for Space Weather", *Adv. Space Res.*, 2016, **58**(10): 1940-1959, https://doi.org/10.1016/j.asr.2016.03.013.

Drob D. P., J. T. Emmert, J. W. Meriwether, J. J. Makela, E. Doornbos, M. Conde, G. Hernandez, J. Noto, K. A. Zawdie, S. E. McDonald, et al.: "An update to the Horizontal Wind Model (HWM): The quiet time thermosphere", *Earth and Space Science*, 2015, **2**: 301-319, doi:10.1002/2014EA000089.

Fuller-Rowell T.: " The thermospheric spoon: A mechanism for the semiannual density variation", *J. Geophys. Res.*, 1998, **103**(A3): 3951-3956.

Sai Gowtam V. and Tulasi Ram S.: "Ionospheric winter anomaly and annual anomaly observed from Formosat-3/COSMIC Radio Occultation observations during the ascending phase of solar cycle 24", *Adv. Space Res.*, 2017

Gulyaeva, T. L., F. Arikan, M. Hernandez-Pajares, and I. S. Veselovsky, North-south components of the annual asymmetry in the ionosphere, *Radio Sci.*, 2014, **49**: 485-496, doi:10.1002/2014RS005401.

Huang Linfeng, Jinsong Wang, Yong Jiang, Jiang Huang, Zhou Chen, Kai Zhao: "A preliminary study of the single crest phenomenon in total electron content (TEC) in the equatorial anomaly region around 120°E longitude between 1999 and 2012", *Adv. Space Res.*, 2014, **54**: 2200-2207, http://dx.doi.org/10.1016/j.asr.2014.08.021.

Jonah O. F. (2013): Analysis of total electron content (TEC) variations obtained from GPS data over South America, Master dissertation of the National Institute for Space Research (INPE), http://urlib.net/8JMKD3MGP7W/3DHJF42

Karpachev A.T. and Gasilov N.A.:"Zonal and meridional wind components derived from intercosmos-19 hmF2 measurements", *Adv. Space Res.*, 2001, **27**(6-7): 1245-1252, https://doi.org/10.1016/S0273-1177(01)00170-3.

Kawamura S.,Balan N. Otsuka Y., and Fukao S.: "Annual and semiannual variations of the midlatitude ionosphere under low solar activity", *J. Geophys. Res.*, 2002, **107**(A8): 1166, doi: 10.1029/2001JA000267.

Liu L., Wan W., Ning B., Pirog O.M. and Kurkin V. I.: "Solar activity variations of the ionospheric peak electron density", *J. Geophys. Res.*, 2006, **111**: 8304, doi:10.1029/2006JA011598.

Liu L., W. Wan, B. Ning, and M.-L. Zhang: "Climatology of the mean total electron content derived from GPS global ionospheric maps", *J. Geophys. Res.*, 2009, **114**: A06308, doi:10.1029/2009JA014244.

Liu L., He M., Yue X., Ning B., Wan W.: "The ionosphere around equinoxes during low solar activity", *J. Geophys. Res.*, 2010, **115**:A09307, doi:10.1029/2010JA015318

Liu H.L., V. A. Yudin, and R. G. Roble: "Day-to-day ionospheric variability due to lower atmosphere perturbations", *Geophys. Res. Lett.*, 2013, **40**: 665-670, doi:10.1002/GRL.50125.

Liu T., Zhang B., Yuan Y. and Li M.: "Real-Time Precise Point Positioning (RTPPP) with raw observations and its application in real-time regional ionospheric VTEC modeling", *J. Geod.*, 2018, **92**:126-1283, https://doi.org/10.1007/s00190-018-1118-2.

Nogueira P.A.B (2013): "Study of characteristics of wave number 4 longitudinal structure and TEC variability over South America", Ph.D. dis-

sertation of the National Institute for Space Research (INPE), < *http* : *//www.inpe.br/pos_graduacao/cursos/geo/arquivos/teses/tese_paulo_alexandre_bronzato_*2013.*pd*

Maruyama T., S. Saito, M. Kawamura, and K. Nozaki: "Thermospheric meridional winds as deduced from ionosonde chain at low and equatorial latitudes and their connection with midnight temperature maximum", *J. Geophys. Res.*, **113**: A09316, doi:10.1029/2008JA013031.

Medeiros R.T., Abdu M.A. and Batista I.S.: "Thermospheric meridional wind at low latitude from measurements of F layer peak height", *J. Geophys. Res.*, 1997, **102**: 14,531-14,540.

Otsuka Y. et al.: "A new technique for mapping of total electron content using GPS network", *Earth Planets Space*, 2002, **54**: 63-70, doi:10.1186/BF03352422.

Pérez-Campos X., V.H. Espíndola, J. Pérez, J. A. Estrada C. Cárdenas Monroy, D. Bello, A. González-López, D. González Avila, M. G. Contreras Ruiz Esparza, R. Maldonado, Y. Tan, I. Rodríguez Rasilla, M.A. Vela Rosas, J. L. Cruz, A. Cárdenas, F. Navarro Estrada, A. Hurtado, A. J. Mendoza Carvajal, E. Montoya-Quintanar, M. A. Pérez-Velázquez: "The Mexican National Seismological Service: An Overview", *Seismological Research Letters*, **89**(2): 318-323, doi: 10.1785/0220170186.

Ren Z., Wan W., Liu L., Chen Y., and Le H. : "Equinoctial asymmetry of ionospheric vertical plasma drifts and its effect on F-region plasma density", *J. Geophys. Res.*, **116**: A02308, doi:10.1029/2010JA016081.

Sai Gowtam V. and Tulasi Ram S.: "Ionospheric winter anomaly and annual anomaly observed from Formosat-3/ COSMIC Radio Occultation observa-

tions during the ascending phase of solar cycle 24", *Adv. Space Res.*, 2017, http://dx.doi.org/10.1016/j.asr.2017.03.017.

Takahashi H.,,: "Ionospheric TEC Weather Map Over South America", *Space Weather*, 2016, **14**: 937-949, doi:10.1002/2016SW001474.

Tsugawa T., S.R. Zhang, A. J. Coster, Y. Otsuka, J. Sato, A. Saito, Y. Zhang, and L. J. Paxton: "Summer-winter hemispheric asymmetry of the sudden increase in ionospheric total electron content and of the O/N 2 ratio: Solar activity dependence", *J. Geophys. Res.*, **112**: A08301, doi:10.1029/2007JA012415.

Unnikrishnan K., Balachandran Nair R., Chandu Venugopal: "Harmonic analysis and an empirical model for TEC over Palehua",*Journal of Atmospheric and Solar-Terrestrial Physics*, 2002, **64**: 1833-1840.

Zhang B., Teunissen P. J. G., Yuan Y., Zhang H. and Li M.: "Joint estimation of vertical total electron content (VTEC) and satellite differential code biases (SDCBs) using low-cost receivers", *J. Geod.*, 2018, **92**:401-413, https://doi.org/10.1007/s00190-017-1071-5.

Zhao B., W. Wan, L. Liu, T. Mao, Z. Ren, M. Wang, and A. B. Christensen: "Features of annual and semiannual variations derived from the global ionospheric maps of total electron content", *Ann. Geophys.*, 2007, **25**: 2513-2527.

Zou L., Rishbeth H., Mulle-Wodarg I.C.F., Aylward A.D., Millward G.H., Fuller-Rowell T.J., Idenden D. W. and Moffett R.J.: "Annual and semiannual variations in the ionospheric F2-layer. I. Modelling", *Ann. Geophys.*, 2000, **18**: 927-944.

Table 1. Solar flux values for 2011 and 2014, using the 81-days running average of daily solar radio flux at 10.7 cm (F10.7A). The columns correspond to: year, phase of solar cycle, average F10.7, minimum of F10.7A, month of occurrence, maximum of F10.7A and month of occurrence.

Year	phase	Avg F10.7A [sfu]	Min F10.7A [sfu]	month	Max F10.7A [sfu]	month
2011	ascending phase	112.9 ± 19.4	87 ± 2.3	Jan, Jul	146 ± 2.6	Oct-Nov
2014	maximum	144.5 ± 12	126 ± 0.9	Jul	163 ± 0.4	Jan

Table 2. Comparison of TEC- and h_mF_2-average during equinoctial and solstitial months corresponding to March-April, June-July, October-November and December of 2011 and 2014.

	March-April		June-July		October-November		December	
Year	TEC (TECu)	h_mF_2 (km)	TEC (TECu)	h_mF_2 (km)	TEC (TECu)	h_mF_2 (km)	TEC (TECu)	h_mF_2 (km)
2011-NH	31.6 ± 5.1	306.6 ± 11.4	28.0 ± 3.1	333.0 ± 1.7	38.6 ± 1.3	290.0 ± 12.2	34.9 ± 1.3	279.2 ± 2.0
2011-SH	28.0 ± 2.2	274.0 ± 11.4	12.4 ± 0.8	237.0 ± 3.3	48.5 ± 7.0	318.3 ± 6.5	52.3 ± 2.3	323.4 ± 1.9
2014-NH	55.2 ± 3.2	341.5 ± 11.7	36.6 ± 2.9	362.8 ± 3.5	40.6 ± 1.8	311.4 ± 12.0	35.5 ± 1.0	299.2 ± 1.7
2014-SH	54.4 ± 8.4	312.0 ± 9.7	17.9 ± 1.2	259.1 ± 3.2	55.4 ± 5.3	336.4 ± 5.2	58.5 ± 1.3	339.0 ± 1.7

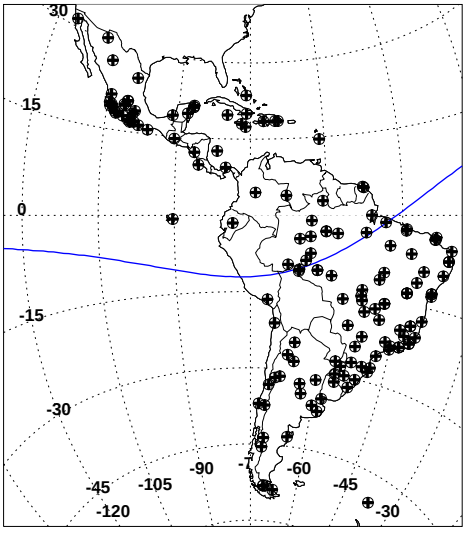

Figure 1. Map of GNSS receivers employed to estimate the vTEC. The blue-line represents the magnetic equator in 2011.

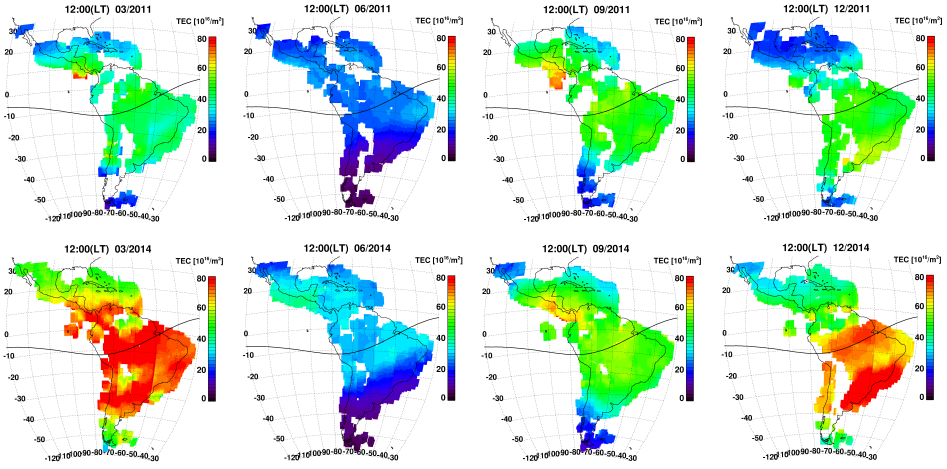

Figure 2. Monthly averaged TEC Maps obtained at 12:00 LT, corresponding to March, June, September and December of 2011 (up) and 2014 (down). Black-line represents the magnetic equator in 2011.

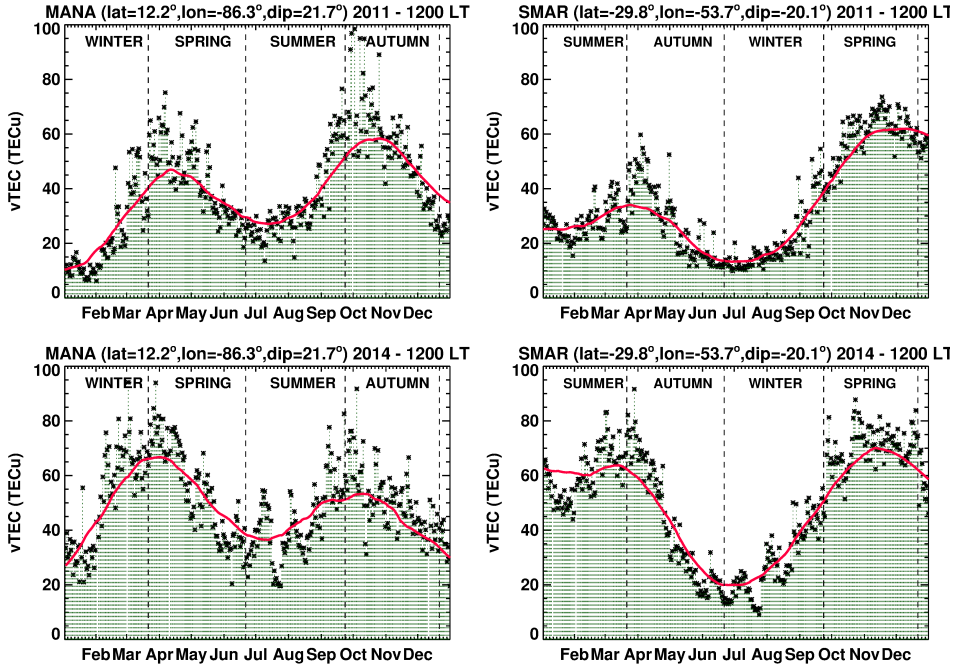

Figure 3. Annual TEC variations at noontime during 2011 (up) and 2014 (down) for two GNSS stations located in the northern (MANA) and southern (SMAR) hemispheres. The red-curves represent the average TEC trend after removing disturbed days and the short-term variations.

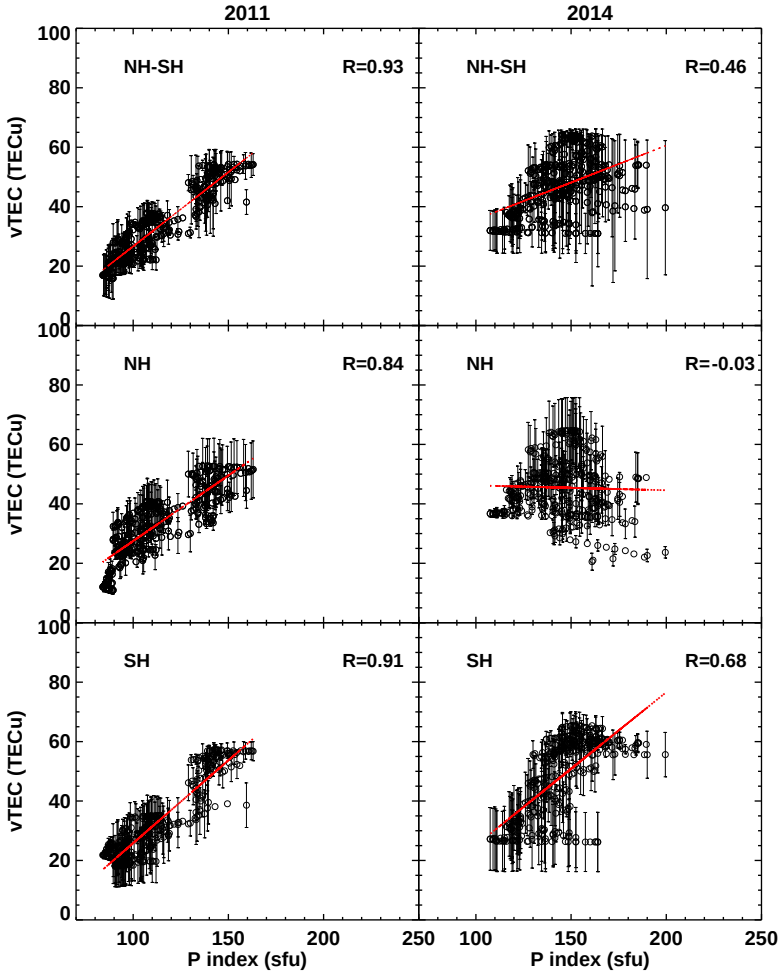

Figure 4. Relation between P index and the average vTEC in the NH and SH for 2011 and 2014. The error bars correspond to the standard deviation of average-TEC values and the red-line is the linear fit.

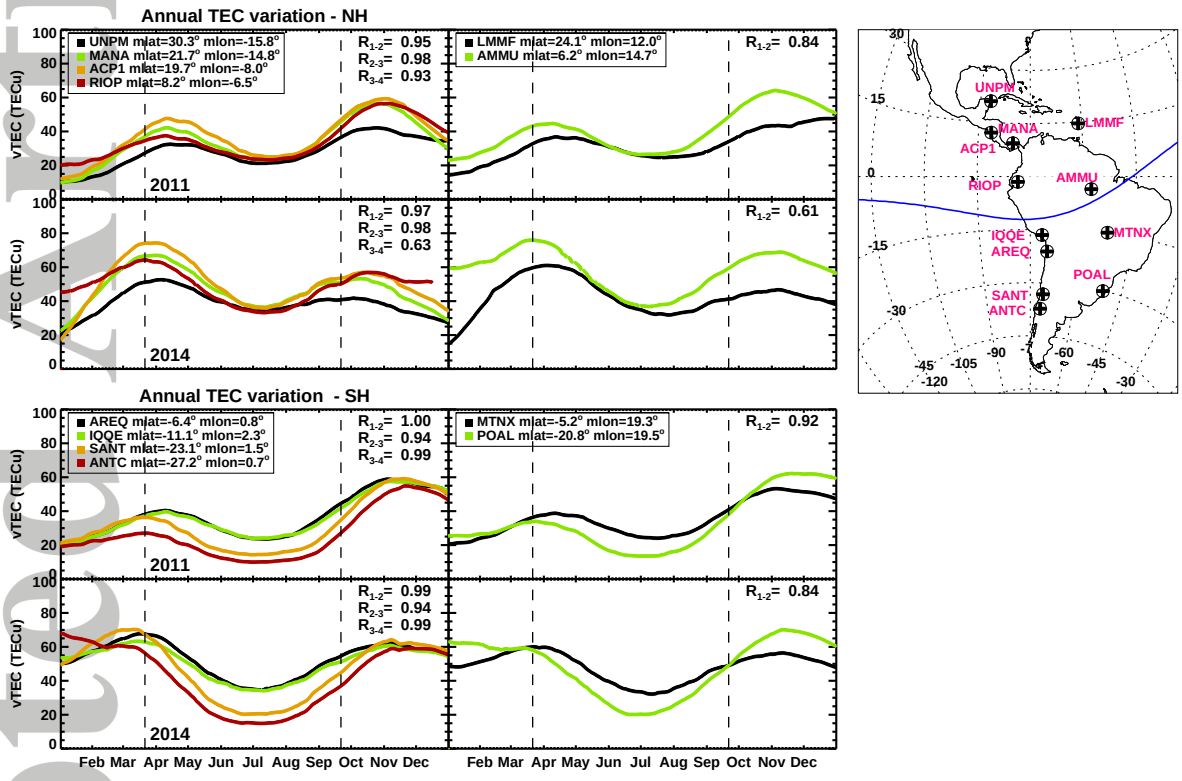

Figure 5. Comparison of the TEC variations obtained at 12:00 LT during 2011 and 2014 for a set of GNSS receivers distribuited at different latitudes. Two longitudinal sectors are employed for the longitudinal comparison. The R-value is the coefficient of linear correlation between GNSS receivers enumerated in the same order as are listed in the label.

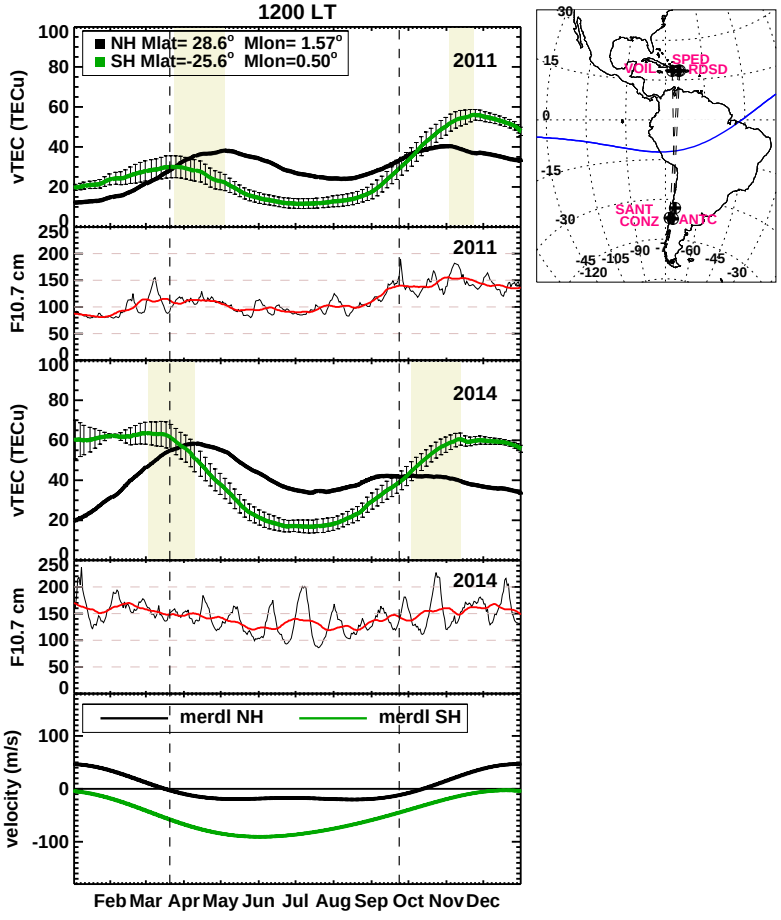

Figure 6. TEC variation at conjugate points during 2011 and 2014. The panels correspond to the TEC variation in the NH and SH, the daily F10.7 and its running average, and the meridional component of neutral wind in the two hemispheres.

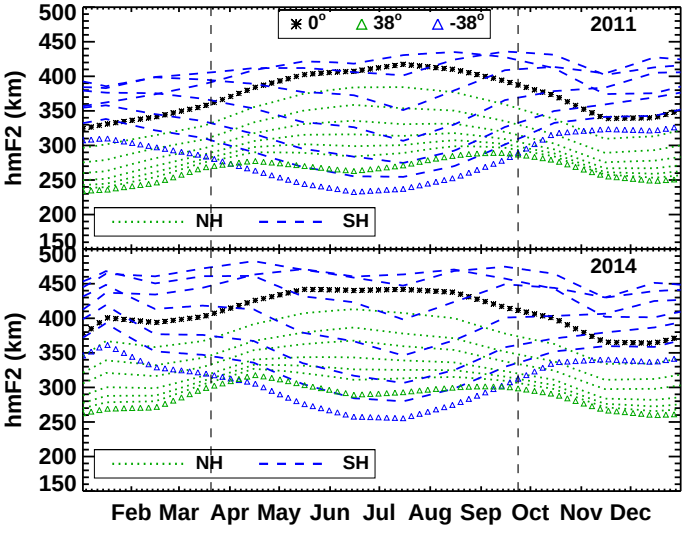

Figure 7. Variation of h_mF_2 at 12:00 LT, obtained from IRI model, during 2011 and 2014. Each of green- and blue-lines corresponds to a particular geographic latitude in the northern and southern hemisphere, respectively. Black-line is representing the h_mF_2 at 0°.